ELSEVIER

Coordination Chemistry Reviews
187 (1999) 303–327

COORDINATION
CHEMISTRY
REVIEWS

Physical properties and mechanisms of formation of nitrous oxide[☆]

William C. Trogler *

Department of Chemistry and Biochemistry, University of California, San Diego, 9500 Gilman Drive, Department 0358, La Jolla, CA 92093-0358, USA

Received 28 July 1998; accepted 11 November 1998

Contents

[☆] Dedicated to Ralph Pearson, for his seminal contributions in inorganic reaction mechanisms and physical inorganic chemistry.

* Tel.: + 1-619-5346175; fax: + 1-619-5345383.
E-mail address: wtrogler@ucsd.edu (W.C. Trogler)

PII: S0010-8545(98)00254-9

Abstract

The role of nitrous oxide (N_2O) in the global nitrogen cycle is discussed. Nitrous oxide is an important trace component of the Earth's atmosphere with a 120-year atmospheric residence time. It exhibits a global warming potential 310 times that of CO_2 on a per molecule basis, and like CO_2, its atmospheric concentration is increasing. Nitrous oxide is produced naturally as a byproduct of nitrification and denitrification. There are also several anthropogenic sources. Structural, physical, spectroscopic, bonding, thermodynamic, and solution properties of NO_2 are reviewed. The reactions known to yield N_2O are surveyed. Fundamental chemical kinetics and mechanisms that lead to its formation are discussed, which emphasize our research involving nitric acid, nitric oxide, and ammonium nitrate as N_2O precursors. These results are discussed in the context of their relevance to biological and environmental chemistry. © 1999 Elsevier Science S.A. All rights reserved.

Keywords: Nitrous oxide; Nitric oxide; Ammonium nitrate; Adipic acid; Kinetics

1. Introduction

Nitrous oxide (dinitrogen oxide, N_2O) is a colorless gas under ambient conditions, which exhibits a slightly sweet odor and taste. It was discovered in 1772 by Joseph Priestley, who called it "diminished nitrous air", from the reduction of NO with iron or iron/sulfur mixtures [1]. Sir Humphrey Davy inhaled N_2O during his medical training in 1799, as part of a study on the physiological effects of several newly discovered gases, and he discovered the ability of N_2O to promote lightheadedness. Public demonstrations rapidly popularized the remarkable effects of N_2O, and laughing gas parties and traveling shows became fashionable. During 1844–1846 the dentists Horace Wells and Gardner Colton demonstrated the useful anesthetic properties of N_2O. About the same time Wells' former partner, William Morton, discovered diethylether was an effective anesthetic. Nitrous oxide continues to be used widely as a mild anesthetic for dental surgery and obstetrics. In major surgical procedures, N_2O is employed as the carrier gas in combination with more potent inhalation general anesthetics, such as halothane. Nitrous oxide is also a trace component of the Earth's atmosphere.

Measurements of the amount of N_2O entrapped in polar ice show that the global concentration of N_2O is higher now than at anytime during the past 45 000 years [2]. After the last ice age the N_2O concentration increased, and then it remained constant (~ 275 ppb) for about 10 000 years until the 19th century. Since then, the N_2O concentration has increased significantly, and this has been attributed to anthropogenic contributions [3]. The atmospheric N_2O concentration now is about 315 ppb, and it has been increasing at a rate of 0.8 ppbv per year [4–10]. There are several reasons why this merits consideration. First, the half-life of atmospheric N_2O is estimated between 110 and 168 years [11,12], and 120 years is the currently accepted value [10]. Even a small rate of increase results in accumulation, and any concentration perturbation that occurs will last for centuries. Second, N_2O is a potent greenhouse gas with a global warming potential about 310 times that of CO_2

[9,10,13]. This must be included in models of future greenhouse warming and in public policy decisions about greenhouse gas reductions. It may be more cost effective to first reduce N_2O emissions instead of CO_2 emissions. Third, N_2O is the main source of stratospheric NO_x, which is an important sink for stratospheric ozone [14]. However, stratospheric NO and NO_2, also react with chlorine oxide radical species in the lower stratosphere and produce stable compounds (e.g. $ClONO_2$) that do not destroy ozone. In the lower stratosphere, the NO derived from N_2O may help reduce ozone depletion from CFC degradation products [15]. The main anthropogenic source of ozone depletion, the CFCs, have been limited by international treaties. As atmospheric levels of CFCs decrease, N_2O would be expected to play an increasing role as an ozone sink. Given the contributions to radiative forcing and stratospheric ozone chemistry, N_2O could someday become problematic if its atmospheric levels continue to increase.

The quantification of N_2O sources is incomplete. Industrial uses of N_2O, as a propellant in canned whipping cream, as a fuel additive in racing cars, and as an anesthetic are small. They cannot account for the significant global increase of 3-4.5 Tg N per year [7–9]. The widespread use of nitrogen fertilizers is suspected to be an important contributor, but this has been difficult to quantify. On a fundamental level, the chemical mechanisms that yield N_2O relate to problems in atmospheric chemistry, biochemistry, and the control of NO_x emissions. Therefore this review will summarize chemical, physical, and mechanistic aspects of N_2O relevant to environmental issues of interest to our research group.

2. Physical properties of nitrous oxide

2.1. *The electronic and geometrical structures of nitrous oxide*

Nitrous oxide is a linear molecule (point group $C_{\infty v}$) that is isoelectronic to CO_2. Bond distances (r_e), determined from rotational spectroscopy measurements, are given in Fig. 1 [16–18]. The electronic structure and geometrical structure can be understood in the context of the valence bond resonance forms shown in Fig. 1.

Both the N=N and the N=O distances in N_2O are reduced from the respective average double bond values of 1.25 and 1.21 Å [19]. The significant shortening of the N=N distance can be attributed to the second contributing resonance form (Fig. 1). Slight shortening of the N=O distance can be attributed to a contraction of orbitals on the central nitrogen atom, because of its positive formal charge in both resonance forms. The opposing charge distribution in the two resonance forms helps explain the relatively low dipole moment (0.161 D) observed for N_2O [20,21].

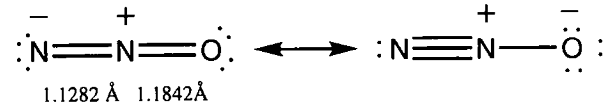

Fig. 1. Resonance forms of nitrous oxide and bond distances, r_e.

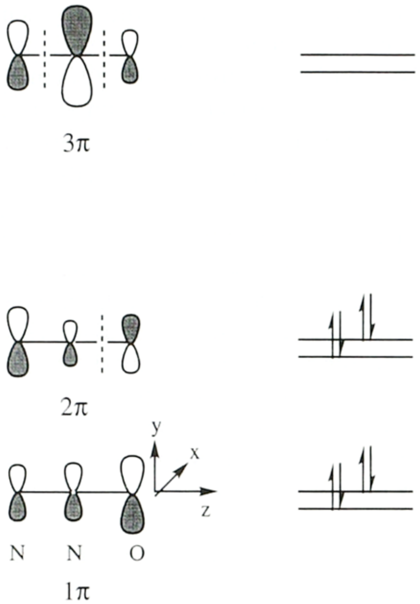

Fig. 2. Allyl-like p frontier orbitals of N_2O. Each degenerate set contains a second orbital in the plane perpendicular to the one depicted that also contains the internuclear axis.

The molecular orbital electronic configuration for N_2O is $(1\sigma)^2(2\sigma)^2(3\sigma)^2(4\sigma)^2(5\sigma)^2(6\sigma)^2(1\pi)^4(7\sigma)^2(2\pi)^4$ [22]. The highest occupied 1π and 2π orbitals each consist of a degenerate (x and y) pair of allyl type π orbitals, as shown in Fig. 2 [23].

In this scheme, the 2π orbital is approximately nonbonding and the lowest unoccupied orbital is the antibonding 3π molecular orbital. Theoretical calculations suggest that the 2π orbital is slightly N–N bonding and N–O antibonding [24,25], which would agree with the shorter N–N distance. The higher electronegativity of oxygen favors a higher composition of its π character in the occupied orbitals and a greater nitrogen π orbital character in the unoccupied 3π antibonding orbital. The highest occupied σ orbital (7σ) is predominantly N–O σ bonding in character [22,26]. Quantitative aspects of the electronic structure calculations will be considered in the section concerning spectroscopic properties.

2.2. Thermodynamic and solubility properties of nitrous oxide

Nitrous oxide liquefies at 183.7 K, freezes at 170.8 K, and the critical temperature and pressure are 36.5°C and 72.4 bar [27,28]. Commercial cylinders of N_2O contain both liquid and gas phases. At S.T.P. the gas has a density of 1.977 g l^{-1} (specific gravity of 1.530 relative to air at 15°C). Traces of N_2O often occur as an impurity in commercial cylinders of NO. Molecular sieves bind N_2O relatively strongly, and are often used in laboratory gas separation schemes. There is recent interest in the use of supercritical fluids, and N_2O may potentially be used as a reactive solvent [29].

Nitrous oxide dissolves in hydrocarbon and alcohol solvents more readily than CO_2. The fat solubility of the gas makes it a useful propellant in whipping cream cans. It also permits N_2O to pass through the hydrophobic blood/brain barrier and act as an anesthetic gas. At a partial pressure of 1.013 bar, the range of reported solubilities for N_2O vary between a maximum mole fraction (x_g) of 0.0305 in pentyl acetate (294.3 K) to a minimum $x_g = 0.00535$ in methanol (298.2 K) [28,30]. In water, N_2O is less soluble than CO_2, since N_2O is a much weaker Lewis acid. The mole fraction of dissolved N_2O at 298.2 K is 4.4×10^{-4}. Added electrolytes further depress the solubility. Two equations for the temperature dependent solubility (273–313 K) of N_2O in pure water have been published [28].

The thermodynamic properties for N_2O at 298.15 K are ΔH_f° of 82.048 kJ mol^{-1}, $\Delta G_f^\circ = 104.172$ kJ mol^{-1}, $S^\circ = 219.979$ J K^{-1} mol^{-1}, and $C_p = 38.838$ J K^{-1} mol^{-1} [18]. The heat of vaporization at the boiling point is 15.55 kJ mol^{-1} and the heat of fusion at the melting point is 6.540 kJ mol^{-1} [27,31]. The high stability of N_2O in the atmosphere, and its relative chemical inertness, must be attributed to kinetics, because it is thermodynamically unstable with respect to the free elements. Decomposition to N_2 and $1/2O_2$ commences at ~600°C. Because N_2O is diamagnetic and the product O_2 is paramagnetic in its ground state, the reaction pathway must proceed by a spin-forbidden route. This results in a high activation energy (~250 kJ mol^{-1}) for the thermal decomposition [32]. There has been considerable interest in the activation of N_2O for oxygen atom transfer reactions to organic substrates. Several examples where oxo transfer to a metal or organic ligand has been reported [33–39], along with one rare example of N=N bond cleavage to form a metal nitrido [40,41].

2.3. Spectroscopic properties of nitrous oxide

2.3.1. Vibrational spectra

The infrared spectrum of N_2O exhibits three strong fundamental absorptions, with superimposed rotational fine structure [42]. The frequencies of the three fundamentals are ν_1 (asymmetric stretch, Σ^+) = 1284.91 cm^{-1}, ν_2 (bending, Π) = 588.77 cm^{-1}, and ν_3 (symmetric stretch, Σ^+) = 2223.76 [43–45]. Two of these (ν_1 and ν_3) also appear in the Raman spectrum. Vibrational spectroscopy provided the initial proof [42] that the molecule adopted an asymmetrical linear structure. The infrared spectrum also exhibits numerous weak absorptions assigned to overtone and combination transitions [1167 cm^{-1} ($2\nu_2$), 1867.5 cm^{-1} ($\nu_1 + \nu_2$), 2461.5 cm^{-1} ($\nu_1 + 2\nu_2$), 2563.5 cm^{-1} ($2\nu_1$), 2798.3 cm^{-1} ($\nu_2 + \nu_3$), 3365.6 ($2\nu_2 + \nu_3$), 3481.2 ($\nu_1 + \nu_3$), 4419.5 ($2\nu_3$), 4734.7 cm^{-1} ($2\nu_1 + \nu_3$)]. In addition, there are several very weak overtones just to lower energy of some stronger fundamentals and combinations. They are found at 579.3, 590.3, 1282, 1828, 1844, 2210, 2776, and 2785 cm^{-1} and arise from molecules thermally populating the ν_2 ($v = 1$) level [42].

Initial attempts to use a simple harmonic valence force field to model the stretching vibrations of N_2O only yield imaginary force constants because of the strong coupling between the N–N and N–O stretches [46]. The more complete quadratic force constants are $f_{11} = 18.01 \times 10^5$ dyn cm^{-1}, $f_{22} = 11.33 \times 10^5$ dyn cm^{-1}, $f_{12} = 1.41 \times 10^5$ dyn cm^{-1}, $f_{\theta\theta} = 0.654 \times 10^{-11}$ erg rad^{-1}, and $f_{\theta r} = 0.486 \times 10^5$ dyn cm^{-1}. The values of f_{11} and f_{22} are reduced slightly from the triple bond values found in N_2 (22.97×10^5 dyn cm^{-1}) [42] and NO (15.5×10^5 dyn cm^{-1}) [47], which is consistent with the structural data (Fig. 1) mentioned earlier.

2.3.2. Ionization potentials and electron affinities of nitrous oxide

The He(I) photoelectron spectrum of N_2O has been determined [48,49]. Energies and qualitative molecular orbital assignments for the outermost valence orbitals are given in Table 1. There have been several valence shell photoionization studies of N_2O that have employed optical excitation or electron energy loss spectroscopy [50–62]. Core binding energies of N_2O have been determined with the use of X-ray photoelectron spectroscopy [63], Auger spectroscopy [64], and synchrotron radiation [65].

Photoionization quantum efficiencies of N_2O have been measured by several methods. Shaw and coworkers have used synchrotron radiation and a double ion chamber technique to obtain data between 975 and 480 Å [66]. They have critically reviewed earlier investigations. After a sharp increase in ionization efficiency at threshold (12.9 eV or $h\nu = 960$ Å), the quantum efficiency shows modulation between 0.5 and 0.8 before rising to a value near 1.0 at wavelengths below 600 Å. The complicated behavior above 600 Å can be assigned to several Rydberg series. Photoionization of N_2O has limited relevance to its atmospheric fate because N_2O undergoes photodissociation at longer wavelength, and the photoionization threshold of N_2O lies above that of O_2, NO, and O [67].

Measurements of the electron affinity of N_2O have been complicated by the anion's tendency to undergo dissociative attachment, yielding O^- and N_2 [68–77]. A Franck–Condon distortion is expected, since N_2O^- is isoelectronic with NO_2 and predicted to possess a bent structure [26,78,79]. This has made measurement of the electron affinity (EA) problematic, and electron transfer from NO^- to N_2O provided the first method for making stable N_2O^- [70,80–82]. A value of 0.22 ± 0.1 eV is favored for the adiabatic EA of N_2O [26,57,83]. The large structural change in N_2O^- is evident in the difference between the adiabatic EA of N_2O and the photodetachment onset at 0.76 ± 0.1 eV in the photoelectron spectrum of

Table 1
Valence shell ionizations of nitrous oxide

Peak energy (eV)	Assignment
12.894	$X^2\Pi_{3/2}$ ionization from 2π
12.931	$X^2\Pi_{1/2}$ionization from 2π
16.388	$A^2\Sigma^+$ ionization from 7σ
17.64	$B^2\Pi$ ionization from 1π
20.105	$C^2\Pi^+$ ionization from 6σ

N_2O^- [84]. This latter value serves as an upper limit for the EA of the neutral species. Negative ion chemistry of N_2O is not thought to be important in the atmosphere, because of the slow kinetics of electron transfer to N_2O [85,86]. This can be attributed to the large Franck–Condon energy barrier expected for electron transfer. Similar factors may explain the relative kinetic inertness of N_2O as an oxidant, even though it is a kinetically strong oxidizing species (being a combination of N_2 and atomic O).

2.3.3. Electronic spectra and molecular orbital theory of nitrous oxide

Early studies of the electronic absorption spectrum of N_2O at several atmospheres in 33 m path length cells [87] suggested that it contained two weak absorptions in the 270–290 nm region. A reinvestigation that determined more accurate cross sections for the lowest electronic transitions failed to find any significant absorption above 260 nm in purified samples [88]. This finding implies that negligible photolysis of N_2O occurs in the troposphere. The erroneous early report of the weak absorptions has appeared in some reviews of N_2O electronic absorption spectra [89,90], which has even led to their proposed assignment in more recent studies [22].

The first diffuse absorption system centered at 182 nm (6.81 eV) has a low oscillator strength ($f = 1.4 \times 10^{-3}$) [23,91]. The first absorption system is attributed to states derived from the valence $(7\sigma)^2(2\pi)^3(3\pi)^1$ electronic configuration, which generates $a^3\Sigma^+$, $b^3\Delta$, $c^3\Sigma^-$, $A^1\Sigma^-$, and $B^1\Delta$ electronic states [22]. Only the $X^1\Sigma^+[(7\sigma)^2(2\pi)^4] \rightarrow A^1\Sigma^-[(7\sigma)^2(2\pi)^3(3\pi)^1]$ transition is both spin and dipole allowed. The weak intensity of the first absorption raises the possibility that it may arise from a vibronically allowed transition $(X^1\Sigma^+[(7\sigma)^2(2\pi)^4] \rightarrow B^1\Delta[(7\sigma)^2(2\pi)^3(3\pi)^1])$.

A second structured absorption system is observed centered at 145 nm (8.52 eV) with an oscillator strength of 7.2×10^{-3} [23,91,92]. This absorption exhibits a long vibrational progression that begins with a 821 cm^{-1} spacing, but ends with the spacing near 448 cm^{-1}. The high degree of anharmonicity would be consistent with an excited state that has a bent (C_s) geometry, and the progression is assigned to the NNO bending mode (compare with $\nu_2 = 589$ cm^{-1}, ground state). This presents a dilemma in the assignment. Walsh diagrams [23] show that the 3π orbital is stabilized the most on bending, which could suggest that this transition be assigned to $X^1\Sigma^+[(7\sigma)^2(2\pi)^4] \rightarrow A^1\Sigma^-[(7\sigma)^2(2\pi)^3(3\pi)^1]$ and the weak 182 nm absorption be assigned to one of the dipole forbidden components. MCSCF/CI calculations [22] predict that a dipole allowed Rydberg transition $X^1\Sigma^+[(7\sigma)^2(2\pi)^4] \rightarrow C^1\Pi[(7\sigma)^2(2\pi)^3(10\sigma\text{-}3s)^1]$ should occur near 8.15 eV; however, this excited state might be expected to resemble N_2O^+ in structure. Spectroscopic studies of the latter species show it to have a linear structure only slightly distorted from the parent neutral species ($\nu_1 = 1126.5$ cm^{-1}, $\nu_2 = 456.8$ cm^{-1}, and $\nu_3 = 1737.7$ cm^{-1}) [17,91]. Other weaker features have been observed in this band system, and the complete assignment of all states in this spectral region is uncertain.

A third intense absorption system lies centered at 128 nm (9.66 eV) with an oscillator strength of 0.36 [23,91,92]. This has been assigned to another Rydberg

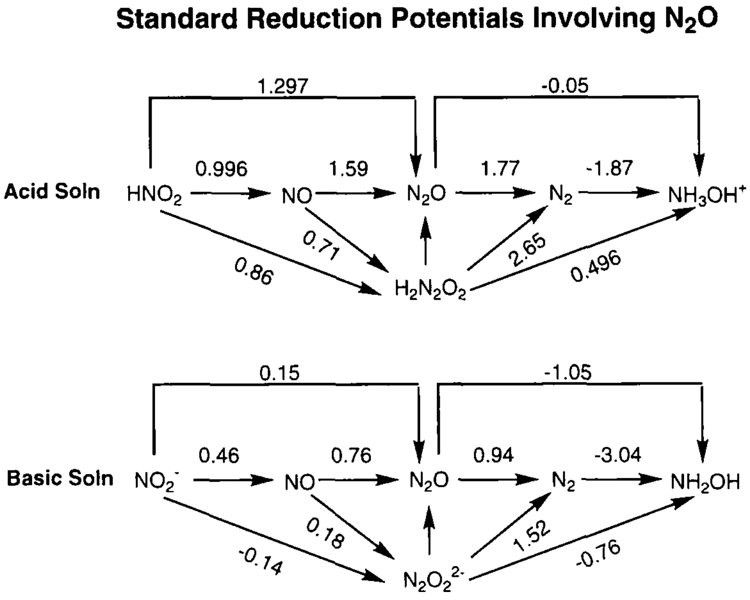

Fig. 3. Redox potential diagram showing standard reduction potentials for reactions that could directly lead to nitrous oxide formation.

type of transition $X^1\Sigma^+[(7\sigma)^2(2\pi)^4] \rightarrow A^1\Sigma^-[(7\sigma)^2(2\pi)^3(4\pi\text{-}3p)^1]$ [22,93]. It should be noted that the dipole allowed $X^1\Sigma^+[(7\sigma)^2(2\pi)^4] \rightarrow A^1\Pi[(7\sigma)^1(2\pi)^4(3\pi)^1]$ transition is also anticipated to occur in this energy region. State assignments and a comparison of earlier MO calculations [94–97] are summarized in the paper of Hopper [22]. There have also been theoretical attempts to quantitatively reproduce the cross sections for photoabsorption and photoionization [25,98,99]. In addition to the lowest absorptions in the ultraviolet and vacuum ultraviolet spectral regions, N_2O has been examined with radiation to 203 eV excitation. These studies bear little on the environmental chemistry of N_2O, and have been summarized elsewhere by Chan and coworkers [93].

2.4. Solution electrochemistry of nitrous oxide

In aqueous solution, the redox inter-conversion between nitrate (N(V)) and ammonium (N(− III)) ions may occur through the intermediacy of N_2O. Half-potentials coupling N_2O with the stable species nitrite, nitric oxide, nitrogen, and hydroxylamine are provided in Fig. 3 [100]. Values are also given for the formation of hyponitrite ($N_2O_2^{2-}$), which contains nitrogen in the same oxidation state (+ 1) as N_2O. Hyponitrous acid (HON=NOH, $pK_{a1} = 6.9$ and $pK_{a2} = 11.6$) [101] is unstable in aqueous solution, and it rapidly decomposes to yield N_2O (Eqs. (1) and (2)). The reaction requires available protons, so $N_2O_2^{2-}$ persists for days in strongly basic solutions (pH 14). Surprisingly, $H_2N_2O_2$ is also stable in strong acid solutions (pH < 3), which suggests that further protonation forms a species, such as $H_3N_2O_2^+$, of enhanced stability.

$$H_2N_2O_{2(aq)} \rightarrow H_2O_{(l)} = N_2O_{(g)} \qquad \Delta G^\circ = -169.0 \text{ kJ mol}^{-1} \qquad (1)$$

$$HN_2O^-_{2(aq)} \rightarrow OH^-_{(aq)} = N_2O_{(g)} \qquad \Delta G^\circ = -129.2 \text{ kJ mol}^{-1} \qquad (2)$$

Based on thermodynamic considerations (Fig. 3), NO is a likely precursor to N_2O from high oxidation state compounds, while hydroxylamine is a likely precursor from reduced nitrogen compounds. Dinitrogen is an extremely unlikely precursor to N_2O for both thermodynamic and kinetic reasons.

Reduction of NO at Pt electrode surfaces has been studied extensively. There is some disagreement about the chemical species involved, which is complicated by the irreversibility of the reaction, the complex wave shapes, and the highly favorable competing reduction of N_2O to N_2 (Fig. 3) [102–108], which is subject to electrocatalysis [109–111]. Early studies of the reduction of N_2O have been summarized [112]. The previous suggested mechanisms for N_2O formation included the reduction of surface NO dimers $(NO)_2$ to hyponitrite ($N_2O_2^{2-}$), followed by protonation and N_2O formation. This was not favored for reduction on Hg electrodes [112]. Here there was evidence for a preequilibrium, postulated to involve protonation of electrode bound NO. Subsequent reduction of the $(NOH^+)_{ad}$ species and dimerization to yield $H_2N_2O_2$ en route to N_2O was favored [112]. Others suggest that protonation of surface bound NO occurs after reduction, and the surface $(NOH)_{ad}$ species then dimerizes [113–115]. Some suggest that in acid solution NO disproportionates, so the species being reduced at the electrode surface is NO^+, which is common to reduction of nitrous acid as well [116]. This seems unlikely, since NO adlayers can be directly observed by FTIR spectroscopy on platinum single crystal electrodes when nitrite is reduced in aqueous solution [117]. Electrogenerative reduction of nitric oxide on platinum [118,119] has been considered as a method for removing NO from exhaust streams [120–124]. Given the importance of NO in chemistry and biology, a better understanding of its aqueous electrochemistry is needed.

3. Reaction mechanisms for the formation of nitrous oxide

3.1. The environmental nitrogen cycle

Nitrogen compounds occur in nature in all the available oxidation states. The most common species relevant to the natural nitrogen cycle are shown in Scheme 1.

For example, nitrogen occurs in soil as nitrate in aerobic environments, but as ammonium or ammonia in anaerobic environments. Redox interconversion between the two extremes is referred to as denitrification and nitrification, as depicted below.

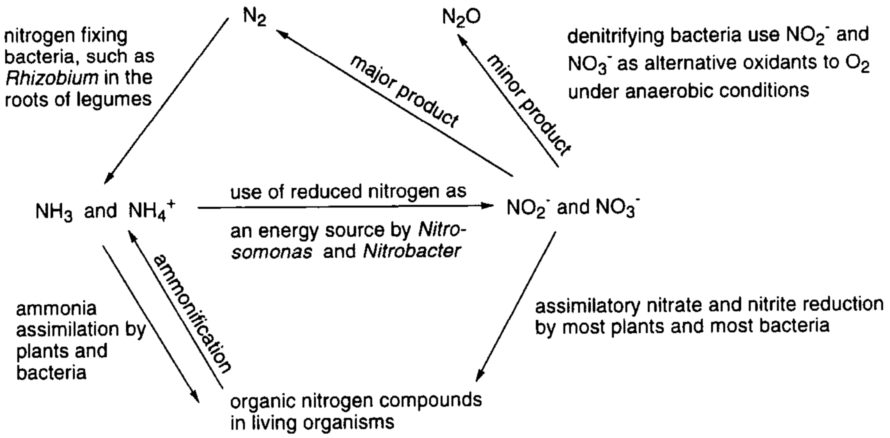

Scheme 1.

$$\overset{+5}{N}O_3^- \Leftrightarrow \overset{+4}{N}O_2 \Leftrightarrow \overset{+3}{N}O_2^- \Leftrightarrow \overset{+2}{N}O \Leftrightarrow \overset{+1}{N}_2O \Leftrightarrow \overset{0}{N}_2 \Leftrightarrow \overset{-3}{N}H_3/NH_4^+$$

denitrification → ← nitrification

The average oxidation state of nitrogen in N_2O places it halfway between the two redox extremes. It is thought that N_2O can be formed by either nitrification or denitrification pathways, but that denitrification predominates [11,125–129]. It is often assumed that oceanic and terrestrial total nitrogen fluxes are in balance in the nitrogen cycle, with the assumption that denitrification can be used to bring the cycles into agreement [130]. It is thought that there are only terrestrial and oceanic sources of N_2O, and that the only sink for N_2O is the stratosphere (photolysis or reaction with $O(^1D)$).

3.2. *Chemical reactions yielding nitrous oxide*

Some of the common chemical reactions that produce N_2O are shown in Scheme 2 [1,101,131,132].

The most common routes to N_2O involve reduction of an oxide of nitrogen. There are relatively few quantitative studies of the detailed mechanisms of these reactions. Because of their relevance to environmental issues, we focused on reactions involving NO, NO_3^-, and NH_4^+. Results of these studies will be summarized.

3.3. *Nitrous oxide from ammonium nitrate*

While the average oxidation state of nitrogen in N_2O is $+1$, it contains a central N in the $+2$ oxidation state and a terminal N atom in the 0 oxidation state. Most synthetic pathways to form N_2O involve the coupling reactions between high and low oxidation state nitrogen compounds. The common laboratory method for

HNO_3 + reductant (NH_4^+, NH_3OH^+, Zn, Sn, $SnCl_2$/HCl, HCOOH, cyclohexanol or cyclohexanone) —> N_2O

NO_2^- + reductant (hydrazine, HN_3, SO_2, Sn^{2+}) —> N_2O

2 NO + reductant (Cu_2O, SO_2, FeO, Fe, S, Fe, Zn, FeS, $SnCl_2$, CuCl, CO, 1,2,3-trihydroxybenzene) —> N_2O

2 NH_2OH + oxidant (Cu^{2+}, HNO_2, Ce^{4+}, Fe^{3+}, Pu^{4+}) —> N_2O

H_2NNO_2 —> $N_2O + H_2O$ (base catalyzed through monoanion)

$H_2N_2O_2$ —> $N_2O + H_2O$ (rapid via monoanion, pH 4-14)

slow disproportionation of NH_2OH in acid and NO in base or acid

4 NH_3OH^+ —> $N_2O + 2\ NH_4^+ + 3\ H_2O + 2H^+$

2 MOH + 4 NO —> 2 $MNO_2 + N_2O + H_2O$ (M = alkali metal)

4 NO + $2H^+$ —> $2NO^+ + N_2O$

Scheme 2.

forming N_2O involves the controlled thermal (~220–250°C) decomposition of ammonium nitrate, Eq. (3) [1]. This reaction is complicated because of several competing processes.

$$NH_4NO_3 \xrightarrow{\Delta} N_2O + 2H_2O \qquad (3)$$

As solid ammonium nitrate is heated, proton transfer begins to evolve gaseous ammonia and nitric acid. The intermediacy of NO_2^+ in the decomposition mechanism has been suggested to occur by autoprotolysis of the released HNO_3 [1,133–136].

Ammonium nitrate is an important fertilizer and over 34 billion kg are produced each year. It is a powerful explosive compound, which detonates with difficulty around 350°C [137]. Because the ultimate product of explosive thermal decomposition (chiefly N_2 and $1/2O_2$) contains excess oxidizing capacity, the explosive yield can be doubled by mixing ammonium nitrate with an additional reductant, such as fuel oil. This mixture is an inexpensive explosive used widely in mining and road construction. Given the ready availability of ammonium nitrate fertilizer, it is also an easily obtained explosive that has been used by terrorists [138]. Traces of chloride salts are known to sensitize the explosive decomposition of solid ammonium nitrate [139–141].

Much ammonium nitrate is produced by the exothermic neutralization of ammonia and nitric acid in titanium pressure reactors where temperatures approach 180–190°C [142]. Therefore, we explored the possible production of N_2O byproduct under conditions similar to those used in the commercial process [143]. The decomposition of aqueous ammonium nitrate at elevated temperatures and pressures was examined as a function of chloride, nitrate, and total acidity. Catalysis requiring both chloride and acid was observed in solutions containing 20% (w/w) NH_4NO_3 at 180°C. Nitrous oxide and dinitrogen were coproduced in a 4:1 ratio below 0.2 M H^+. Dinitrogen formation correlated with the production of additional acidity by the reaction of Eq. (4).

$$5NH_4NO_3 \rightarrow 4N_2 + 2HNO_3 + 9H_2O \tag{4}$$

The decomposition reaction's second-order dependence on $[H^+]$ is consistent with the reversible formation of NO_2^+ as a key step. Incorporation of ^{18}O into the N_2O product is observed as for organic nitrations [144]. The observed inverse deuterium isotope effect of approximately two further supports this conclusion. Inverse isotope effects usually reflect the influence of the zero point energy differences on equilibrium constants [145]. Thus, DNO_3 is less dissociated than HNO_3 because the O–D bond is slightly stronger than the O–H bond. The ultimate product of nitric acid dehydration is water and the greater stability of D_2O over H_2O further favors NO_2^+ formation. Autoprotolysis of nitric acid might not be expected at the modest acid concentrations employed; however, at 180°C the K_a of nitric acid is estimated to be 0.1–1.0 from literature data [146]. Nitric acid is the weakest of the 'strong acids' and the rapid decrease in the dielectric constant of water with increasing temperature is enough to cause it to become incompletely ionized at temperatures above ~ 120°C.

A novel mechanism based on the intermediacy of NO_2Cl was suggested (Scheme 3) for the chloride catalysis in contrast to the radical-based pathways previously proposed [133] for molten NH_4NO_3 decompositions. It also differs from a mechanism proposed for the chloride-catalyzed decomposition of ammonium nitrate in 1–8 M HNO_3 solutions, which invoked the initial formation of HOCl [147]. Isotope labeling experiments using $^{15}NH_4NO_3$ yield $^{15}N{=}N{=}O$ labeled N_2O and the dinitrogen products $^{15}N{\equiv}^{15}N$ and $N{\equiv}^{15}N$ in a 1:3 ratio. Decomposition of $NH_4^{15}NO_3$ produces only $N{=}^{15}N{=}O$ and $N{\equiv}^{15}N$. The distribution of isotopes in N_2O product

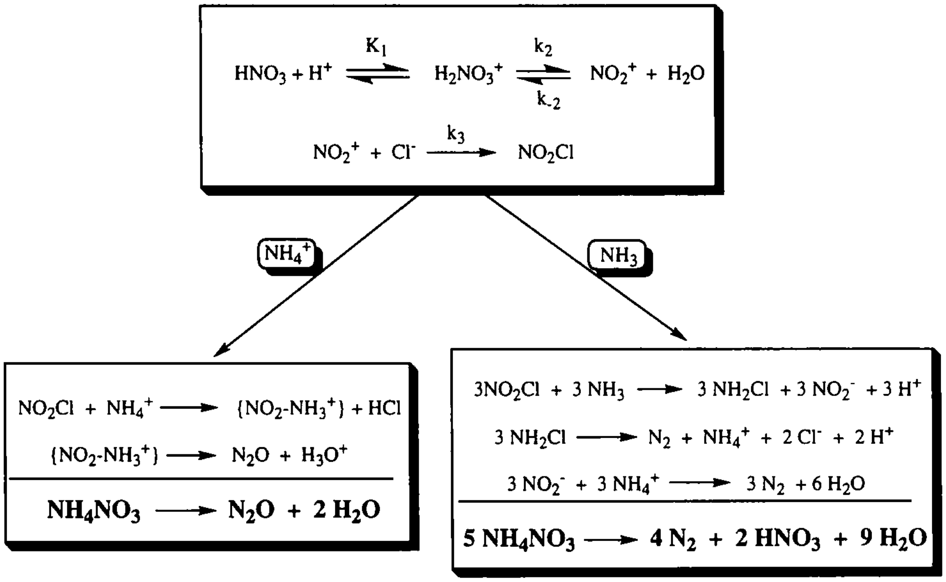

Scheme 3.

is the same as had been observed for decomposition of the solid [148]. The unusual isotope distribution in the N_2 product agrees with the reaction mechanism shown in Scheme 3. This scheme explains the second order proton dependence of the initial rates. The k_3 step explains the catalytic role of chloride. The branching of the mechanism, with the NO_2Cl/NH_4^+ reaction yielding N_2O and the NO_2Cl/NH_3 reaction producing N_2, explains the excellent linear dependence of the N_2O/N_2 product ratio on the proton concentration. The pathway for dinitrogen production was based on the known ability of NO_2Cl to chlorinate ammonia [149]. A steady state treatment of NO_2^+ yields the kinetics expression of Eq. (5).

$$\text{rate} = (k_2k_3[\mathrm{Cl}^-][\mathrm{H_2NO_3^+}])/(k_{-2} + k_3[\mathrm{Cl}^-]) \qquad (5)$$

Because $[HNO_3]$ can be approximated as $[H^+][NO_3^-]/K_{a(HNO_3)}$, this rate expression is consistent with the second-order acid dependence and the first-order chloride dependence observed for the initial rates of decomposition.

The pathway that generates N_2 also produces protons, which appear in the rate law. Thus, the reaction is product catalyzed and the autocatalytic shape to the entire reaction curve can be reproduced with the kinetic parameters derived from the initial rate studies. The kinetics experiments were conducted in 20% (w/w) solutions of ammonium nitrate. At concentrations above 50% the rates accelerate dramatically and it is not necessary to have acid present initially for the reaction to accelerate. Apparently the traces of HNO_3 produced when NH_4NO_3 is heated, as well as the protons accompanying N_2 production, are sufficient to promote a rapidly accelerating decomposition. Concentrated solutions also favor dehydration of nitric acid due to the high level of salts. The temperature dependence is also very steep, with the reaction approaching explosive rates in concentrated solutions above 200°C. The exothermic character of the decomposition would be expected to cause a temperature increase in concentrated solutions, which would further accelerate decomposition.

These mechanistic findings bear on the industrial preparation of NH_4NO_3, and suggest conditions under which N_2O emissions from fertilizer manufacturing might be important to the global N_2O budget. The high efficiency of chloride catalysis also suggest a plausible mechanism for a 1994 accidental explosion at Terra Industries [150]. There an 85–90% solution of ammonium nitrate containing chloride contaminated nitric acid was heated to ~220°C during steam cleaning of the neutralizer. The greatest industrial disaster in the US (Texas City, 1947) [151] occurred when a ship hold laden with ammonium nitrate fertilizer caught fire. Whether an influx of salt water from fire fighting efforts or from breaches in the hull helped initiate the explosion in this incident (and in several other accidental shipboard explosions) remains an interesting question.

3.4. Nitrous oxide from nitrate reduction during adipic acid production

Estimated excess N_2O emissions of ~1 Tg N per year in the Northern Hemisphere have suggested the presence of unknown industrial N_2O sources [5]. This was puzzling because nitrous oxide's commercial uses as a dental anesthetic (laughing gas) and a propellant in canned whipping cream were too small to be significant. In

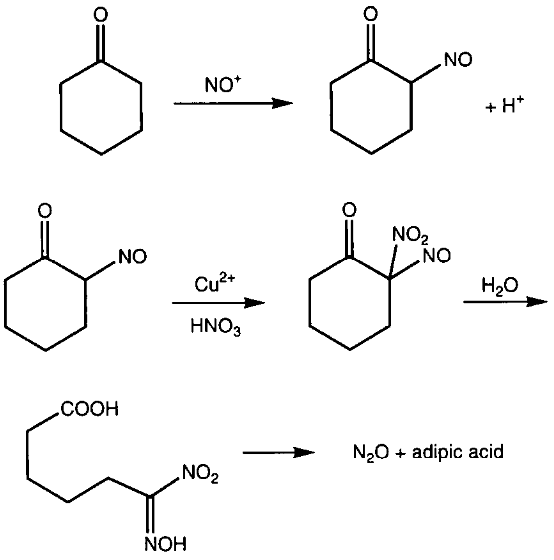

Scheme 4.

1990, we became aware that N_2O is produced as a byproduct from the manufacture of adipic acid for the synthesis of 6,6-nylon. Oxidation of cyclohexanol/cyclohexanone mixtures with 50% nitric acid charged with VO_3^- and Cu^{2+} catalysts evolved about 1 mole of N_2O gas for each mole of adipic acid isolated [152]. By using the known yearly production of adipic acid it is estimated that 0.4–0.6 Tg N per year are produced as a byproduct of this process. The mechanism responsible for this reaction is speculative; however, the stoichiometry is consistent with one proposal shown in Scheme 4 [153].

These industrial emissions account for about half the difference seen in N_2O emission rates from the Northern and Southern Hemispheres. Two months after publication of this article [152] worldwide nylon producers voluntarily committed to a 5-year phase out of N_2O emissions. An EPA 'Green Nylon' program was created to help the US meet 10% of its target greenhouse gas emission reduction goals by placing controls on adipic acid manufacturing facilities. This has also led to modifications in commercial adipic acid synthesis. The most recent advance has been an industrial process, which originated at the Boreskov Institute of Catalysis and was recently commercialized by Solutia [154–160]. It captures N_2O from the adipic acid process and uses it for the one-step catalytic oxidation of benzene to produce phenol. There has been considerable interest in the mechanism for N_2O decomposition on surfaces because of the relationship to this catalytic process, as well as to the catalytic destruction of N_2O emissions [161–210].

3.5. Nitrous oxide from reductive coupling of nitric oxide

On a more fundamental level we have explored metal-catalyzed mechanisms that might be important in N_2O forming reactions from NO as the immediate precursor.

The palladium–copper catalyzed reduction of nitric oxide (NO) to nitrous oxide (N_2O) with carbon monoxide (Eq. (6)) was of particular interest because of its gross similarity to the Wacker process [211,212]. This reaction is also significant because it may resemble a pathway by which NO is reduced to dinitrogen in automotive catalytic converters. As noted earlier, N_2O is thermodynamically unstable and it could be an intermediate along catalytic NO decomposition pathways that yield N_2 and H_2O/O_2.

$$2NO + CO \xrightarrow{[PdCl_4]^{2-} \cdot CuCl_2} N_2O + CO_2 \tag{6}$$

A similar catalytic system was reported based on Pt(II) and Cu(I), and its kinetics and reaction mechanism have been carefully studied [213]. In this system, the major species present during the catalytic cycle was shown to be $[PtCl_3(CO)]^-$. This complex reacts with NO and water according to a rate law first order in the NO partial pressure (P_{NO}) and in [CuCl] to yield N_2O. The key intermediate involved in the N_2O forming step was postulated to be a Pt(I) species, $[PtCl_2(NO)]^{2-}$. A key difference was noted because N_2O evolution is simultaneous with CO disappearance, whereas in the palladium system most CO disappears before N_2O formation commences.

Particularly intriguing in the palladium-catalyzed reaction was the report of a yellow intermediate ($\lambda_{max} = 436$ nm) postulated to be the active catalyst. It was thought to be a soluble Pd/Cu nitrosyl species [212]. In initial stoichiometry experiments we found that the yellow intermediate built up rapidly from one equivalent of NO, CuCl, and $[PdCl_4]^{2-}$. However, the same species could be produced in the absence of copper by adding NO to a suspension of Pd^0 in HCl solution. Addition of Ph_4AsCl and extraction of this solution with dichloromethane led to the identification of blue *trans*-$[Ph_4As]_2[Pd_2Cl_4(NO)_2]$ ($\nu_{NO} = 1701$ and 1623 cm^{-1}) [214]. From the stoichiometry experiments (1 mol $[PdCl_4]^{2-}$, 1 mol reducing equivalent, 1 mol NO) and the observation of the blue dimer on extraction, it seemed likely that a monomer–dimer equilibrium similar to that undergone by the parent complex $[PdCl_4]^{2-}$ was occurring (Eqs. (7) and (8)).

aqueous ↔ nonaqueous

$$2[PdCl_4]^{2-} \leftrightarrow 2Cl^- + [Pd_2(\mu\text{-}Cl)_2Cl_4]^{2-} \tag{7}$$

$$2[PdCl_3NO]^{2-} \leftrightarrow 2Cl^- + trans\text{-}[Pd_2(\mu\text{-}Cl)_2Cl_2(NO)_2]^{2-} \tag{8}$$

Although the yellow monomeric nitrosyl was too unstable to isolate, it exhibits a strong ν_{NO} at 1662 cm^{-1} in D_2O/DCl [215]. This is exactly the average of the NO stretching frequencies for the symmetric and asymmetric stretches in the blue dimer, which argues for a common metal oxidation state and coordination environment in both compounds. It is surprising that such a simple coordination complex, $[PdCl_3NO]^{2-}$, was unknown. Since this complex forms rapidly during the catalytic reaction between NO and CO, it suggests that the next step is rate determining. We inferred that the known reaction between CO and $[PdCl_4]^{2-}$ provided Pd^0 which, by analogy to the Wacker process, reduced Cu^{2+} to Cu^+ and regenerated $[PdCl_4]^{2-}$. Thus, the catalytic cycle can be more simply studied without CO according to Scheme 5.

The rate-determining step for N_2O formation was first order in the palladium concentration and NO partial pressure. The cuprous chloride dependence was first-order below 0.1 M; at higher concentrations saturation kinetics were observed. The rate of reaction was also independent of H^+ and Cl^- concentrations. These results are consistent with the initial reversible attack (k_1/k_{-1}) of free NO on the bound nitrosyl of $[PdCl_3NO]^{2-}$ yielding $[PdCl_3(N_2O_2)]^{2-}$, which is then reduced by Cu(I) (k_2) to generate products and recycle the palladium, as shown in Scheme 5.

While the structure of the species formed by addition of the second NO is unknown, we speculate that it occurs by electrophilic attack of free NO on the lone pair of the coordinated bent nitrosyl. The low NO stretching frequency in $[PdCl_3NO]^{2-}$ suggests a bent Pd–N–O geometry with a nucleophilic lone pair on nitrogen. Subsequent addition of the second reducing equivalent (after N–N coupling) would yield hyponitrite, an unstable species that rapidly decomposes to N_2O, as noted earlier. Addition of NO to the lone pair of a bound NO had been suggested previously for cobalt nitrosyls [216–218]. A k_1 value of $(6.0 \pm 0.4) \times 10^{-6}$ $(\text{torr})^{-1}$ s^{-1} at 20°C was calculated, with a k_1/k_2 ratio of 0.116 ± 0.004 M. The rate of N_2O evolution from the catalytic system using CuCl as the reductant was 93% the rate of N_2O evolution by Eq. (6), which shows that this scheme quantitatively models the rate limiting step in the complete CO/NO catalytic process [215].

Nitric oxide is thought to be an obligatory intermediate to N_2O in the biological denitrification pathway [129]. Functional models of copper nitrite reductase have been developed that reduce NO to N_2O [219–224]. The reaction employs either

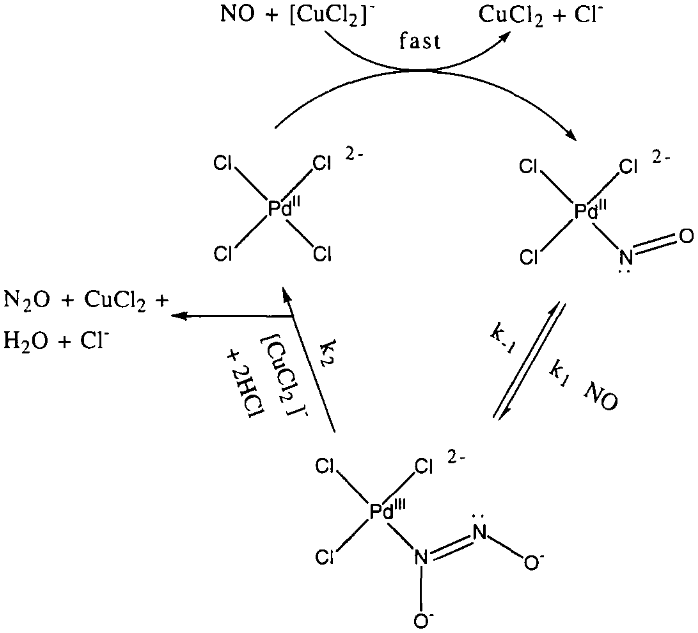

Scheme 5.

mononuclear or dinuclear Cu(I) complexes, and one study suggests that a Cu(II)($N_2O_2^{2-}$)Cu(II) species is a likely intermediate [222]. Attack of free NO on complexed NO has been suggested in several proposed N_2O generation schemes [223,225,226]. The mechanism of NO binding, one-electron reduction, NO coupling, one-electron reduction observed for the homogeneous Pd(II)/Cu(I) catalytic system may serve as a model for N_2O formation in several biological systems. The parallel between the nitric oxide reductase activity of cytochrome *c* oxidases, which proceed by two-electron reduction (provided by Cu(I)) of a heme bound nitrosyl, was drawn [215]. Although a two-electron reduction to a metal nitrido complex had been suggested [227], we proposed that a stepwise mechanism would provide a lower energy pathway [215]. Similarly, for the eukaryotic denitrification enzyme P450nor isolated from the fungus *Fusarium oxysporum* [228–232], a mechanism involving two-electron reduction of an intermediate nitrosyl complex was proposed originally [232]. However, this enzyme cannot catalyze the monooxygenase reaction, and we suggested that it too might involve a hyponitrite intermediate. The hyponitrite mechanism has now been considered as a better model for the mechanism of NO reduction by P450nor [231], and it may be of broad biological significance. The advantage to this mechanism over the alternative suggestion of reductive coupling of 2NO at a single metal center [129] is that it can explain N_2O formation in heme enzymes where *cis* coordination is unlikely. Of course, it is always possible that several mechanistic pathways are employed in biological systems.

3.6. Catalyzed disproportionation of nitric oxide under basic conditions

A heterogeneous Pd^0 on activated charcoal catalyst was examined in 3 M NaOH [233]. The activity of this catalyst for removing NO from the headspace above the solution was high, and control reactions showed little activity in the filtrate from these solutions. Control experiments showed that the disproportionation reaction of Eq. (9) is catalyzed weakly by a slurry of activated carbon, and greatly accelerated by palladium-treated activated carbons. Mass balance experiments are consistent with the stoichiometry of Eq. (9).

$$4NO + 2OH^- \rightarrow N_2O + 2NO_2^- + H_2O \tag{9}$$

The rate can be followed conveniently by monitoring the evolution of N_2O, which established true catalytic turnover, with no loss in activity after hundreds of turnovers. The catalytic activity with supported Pd^0 or Pt^0 on carbon is 2–4 turnovers min^{-1} mol Pd^{-1} or Pt^{-1} at 21°C. Catalysts prepared from adsorbing Pt(II) and Pd(II) salts on activated carbon have low catalytic activities and the adsorbed metal ions must be reduced to the metallic state under H_2 before high activity is observed. Other supports, such as alumina or silica can be used, but unlike activated carbon, the alumina and silica possess no catalytic activity alone. A suspension of freshly reduced Pd^0 (prepared by CO addition to $[PdCl_4]^{2-}$) colloid also exhibits catalytic activity in basic aqueous solution. In addition, we have recently found that other metals, such as gold, are catalysts for this process.

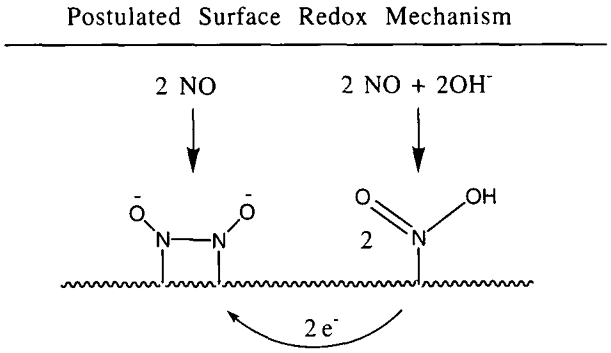

Scheme 6.

The Pd/C catalyzed reaction ceases when the pH falls to about 6–6.5, which was interpreted as being suggestive of the presence of a hyponitrite intermediate. While the reaction of Eq. (9) is thermodynamically favorable at all accessible pH values (Fig. 3), it would be expected to become unfavorable according to the Nernst equation at pH 6.3 if $H_2N_2O_2$ were a requisite intermediate. Since all the catalytically active solids (C, Pt, Pd, and Au) are electrical conductors, we postulated a galvanic surface mechanism (Scheme 6) similar to that involved in corrosion. While the known ability of NO to dimerize on carbon surfaces suggests that dimeric NO species are involved, reduction of NO to a HNO intermediate is also possible.

Formation of N_2O can be blocked by the addition of as little as 1–2% O_2 to the reaction gases. These experiments were conducted at low partial pressures of NO (below 5000 ppm) so the direct reaction between NO and O_2 is slower (due to the second order NO dependence) than the catalytic process. This suggests that surface bound O_2, which is a stronger oxidant than NO dimer, can compete as the electron acceptor and the product can be directed entirely to NO_2^- formation.

This offers a new catalytic approach for NO scrubbing from exhaust gases. The catalysts are not poisoned by SO_2 and the basic solution simultaneously removes SO_x. Current post-combustion technologies for controlling stack gas emissions are especially problematic for coal-fired utilities. Selective catalytic reduction (SCR) of NO by NH_3 at 300–400°C is the preferred NO_x control method [234]; however, difficulties with fly ash poisoning, precipitation of ammonium sulfate, and high capital and operating expenses have prompted a search for other methods. Selective non-catalytic reduction (SNCR) of NO_x to N_2, employing ammonia or urea is used infrequently, and it requires the costly reheating of stack gases to temperatures in the range 800–1200°C. The decomposition of NO to N_2 and O_2 with Cu-doped ZSM-5 zeolites and related transition metal exchanged zeolites has been explored [174,235–248]; however, this process is not yet viable for stationary combustion sources.

Non-catalytic oxidation/reduction and absorption techniques (chemical scrubbing) have the advantage of being able to eliminate both NO_x and SO_x simultaneously [249,250]. The primary difficulty with their industrial application has been the low solubility of NO in aqueous solution. Nitric oxide constitutes 90–95% of the NO_x present in typical flue gas streams, and one solution has been to preoxidize NO to NO_2 before the scrubber. Because of the second order dependence of the direct oxidation of NO with O_2, the reaction is inefficient at the low NO concentrations encountered in exhaust gases. Other approaches considered for treating NO in aqueous scrubbers include adding heavy-metal chelators for nitric oxide and adding yellow phosphorous emulsions and O_2 to oxidize nitric oxide to a combination of nitrite and nitrate salts [251–253]. Metal on carbon catalysts offer the advantage of an absorptive method for removing NO and a surface catalyzed oxidation to fix it as a solution species. Turnover rates will need to be improved significantly before it could be applied.

Acknowledgements

Support of our research in the chemistry of nitrogen oxides by the US National Science Foundation is gratefully acknowledged.

References

[1] J.W. Mellor, A Comprehensive Treatise on Inorganic and Theoretical Chemistry, vol. VIII, Wiley, New York, 1922.
[2] M. Leuenberger, U. Siegenthaler, Nature 360 (1992) 449.
[3] W.C. Trogler, J. Chem. Educ. 72 (1995) 973.
[4] M.A.K. Khalil, R.A. Rasmussen, Tellus 35B (1983) 161.
[5] M.A.K. Khalil, R.A. Rasmussen, J. Geophys. Res. Atm. 97 (1992) 14651.
[6] R.F. Weiss, J. Geophys. Res. 86 (1981) 7185.
[7] The Intergovernmental Panel on Climate Change, J.T. Houghton, G.J. Jenkins, J.J. Ephraums, Climate Change: The IPCC Scientific Assessment, Cambridge University Press, Cambridge, 1990.
[8] J.T. Houghton, B.A. Callander, S.K. Varney, Climate Change 1992: The Supplementary Report to the IPCC Scientific Assessment, Cambridge University Press, Cambridge, 1992.
[9] J.T. Houghton, L.G. Meira Filho, J. Bruce, H. Lee, B.A. Callander, E. Haites, N. Harris, K. Maskell, Climate Change 1994. Radiative Forcing of Climate Change and An Evaluation of the IPCC IS92 Emission Scenarios, Cambridge University Press, Cambridge, 1994.
[10] J.T. Houghton, Climate Change 1996: The Science of Climate Change, Cambridge University Press, Cambridge, 1996.
[11] R.J. Cicerone, J. Geophys. Res. Atm. 94 (1989) 18265.
[12] R. Prinn, D. Cunnold, R. Rasmussen, P. Simmonds, F. Alyea, A. Crawford, P. Fraser, R. Rosen, J. Geophys. Res. Atm. 95 (1990) 18369.
[13] O. Badr, S.D. Probert, Appl. Energy 44 (1993) 197.
[14] T.E. Graedel, P.J. Crutzen, Atmospheric Change: an Earth System Perspective, Freeman, New York, 1993.
[15] P.O. Wennberg, R.C. Cohen, R.M. Stimpfle, J.P. Koplow, J.G. Anderson, R.J. Salawitch, D.W. Fahey, E.L. Woodbridge, E.R. Keim, R.S. Gao, C.R. Webster, R.D. May, D.W. Toohey, L.M. Avallone, M.H. Proffitt, M. Loewenstein, J.R. Podolske, K.R. Chan, S.C. Wofsy, Science 266 (1994) 398.
[16] J.L. Griggs, K.N. Rao, L.H. Jones, R.M. Potter, J. Mol. Spectrosc. 25 (1968) 24.
[17] J.H. Callomon, F. Creutzberg, R. Soc. (Lond.) Phil. Trans. 277A (1974) 157.

[18] M.W. Chase, C.A. Davies, J. Downey Jr., D.J. Frurip, R.A. McDonald, A.N. Syverud, J. Phys. Chem. Ref. Data. (Suppl. 1) 14 (1985) 1554.
[19] J.E. Huheey, Inorganic Chemistry, Principles of Structure and Reactivity, Harper&Row, New York, 1983.
[20] D. Bellert, T. Buthelezi, V. Lewis, K. Dezfulian, P.J. Brucat, Chem. Phys. Lett. 240 (1995) 495.
[21] K. Mogi, T. Komine, K. Hirao, J. Chem. Phys. 95 (1991) 8999.
[22] D.G. Hopper, J. Chem. Phys. 84 (1984) 4290.
[23] J.W. Rabalais, J.M. McDonald, V. Scherr, S.P. McGlynn, Chem. Rev. 71 (1971) 73.
[24] K. Jug, J. Am. Chem. Soc. 100 (1978) 6581.
[25] D.A.L. Kilcoyne, S. Nordholm, N.S. Hush, Chem. Phys. 107 (1986) 225.
[26] D.G. Hopper, A.C. Wahl, R.L.C. Wu, T.O. Tiernan, J. Chem. Phys. 65 (1976) 5474.
[27] O. Knacke, O. Kubaschewski, K. Hesselmann, Thermochemical Properties of Inorganic Substances, Part II, Springer-Verlag, Berlin, 1991.
[28] P.G.T. Fogg, W. Gerrard, Solubility of Gases in Liquids. A Critical Evaluation of Gas/Liquid Systems in Theory and Practice, Wiley, New York, 1991.
[29] P. Jessop, Topics Catal. 5 (1998) 95.
[30] C.J. Chang, C.-Y. Chen, H.-C. Lin, J. Chem. Eng. Data 40 (1995) 850.
[31] I. Barin, F. Sauert, E. Schultze-Rhonhof, W.S. Sheng, Thermochemical Data of Pure Substances, Part II, VCH, Wiesbaden, 1989.
[32] I.R. Beattie, Mellor's Comprehensive Treatise on Inorganic and Theoretical Chemistry, Supplement 2, Part 2, Nitrogen, Longmans, London, 1967, p. 189.
[33] M. Dionne, J. Jubb, H. Jenkins, S. Wong, S. Gambarotta, Inorg. Chem. 35 (1996) 1874.
[34] A. Kaplan, R.G. Bergman, Organometallics 16 (1997) 1106.
[35] K.M. Koo, G.L. Hillhouse, A.L. Rheingold, Organometallics 14 (1995) 456.
[36] A. List, K. Koo, A.L. Rheingold, G.L. Hillhouse, Inorg. Chim. Acta 270 (1998) 399.
[37] P.T. Matsunaga, G.L. Hillhouse, A.L. Rheingold, J. Am. Chem. Soc. 115 (1993) 2075.
[38] P.T. Matsunaga, J.C. Mavropoulos, G.L. Hillhouse, Polyhedron 14 (1995) 175.
[39] G.A. Vaughan, G.L. Hillhouse, A.L. Rheingold, J. Am. Chem. Soc. 112 (1990) 7994.
[40] C.E. Laplaza, A.L. Odom, W.M. Davis, C.C. Cummins, J.D. Protasiewicz, J. Am. Chem. Soc. 117 (1995) 4999.
[41] A.R. Johnson, W.M. Davis, C.C. Cummins, S. Serron, S.P. Nolan, D.G. Musaev, K. Morokuma, J. Am. Chem. Soc. 120 (1998) 2071.
[42] G. Herzberg, Molecular Spectra and Molecular Structure. II. Infrared and Raman Spectra of Polyatomic Molecules, Van Nostrand Reinhold, New York, 1945.
[43] J.L. Griggs, K.N. Rao, L.H. Jones, R.M. Potter, J. Mol. Spectrosc. 25 (1968) 24.
[44] J.L. Griggs, K.N. Rao, L.H. Jones, R.M. Potter, J. Mol. Spectrosc. 18 (1965) 212.
[45] J. Pliva, J. Mol. Spectrosc. 27 (1968) 461.
[46] W.G. Penny, G.B.B.M. Sutherland, Proc. R. Soc. (Lond.) A156 (1936) 654.
[47] D.C. Harris, M.D. Bertolucci, Symmetry and Spectroscopy. An Introduction to Vibrational and Electronic Spectroscopy, Dover Publications, New York, 1978.
[48] C.R. Brundle, D.W. Turner, Int. J. Mass Spectrom. Ion Phys. 2 (1969) 195.
[49] D.W. Turner, D.P. May, J. Chem. Phys. 46 (1967) 1156.
[50] J. Berkowitz, J.H.D. Eland, J. Chem. Phys. 67 (1977) 2740.
[51] T. Cvitas, L. Klasinc, B. Kovac, R. McDiarmid, J. Chem. Phys. 79 (1983) 1565.
[52] P.M. Dehmer, J.L. Dehmer, W.A. Chupka, J. Chem. Phys. 73 (1980) 126.
[53] W. Domcke, L.S. Cederbaum, J. Schirmer, W. von Niessen, C.E. Brion, K.H. Tan, Chem. Phys. 40 (1979) 171.
[54] J.H.D. Eland, Mol. Phys. 40 (1980) 917.
[55] R.H. Heubner, R.J. Celotta, S.R. Mielczarek, C.E. Kuyatt, J. Chem. Phys. 63 (1975) 4490.
[56] R.I. Hall, A. Chutjian, S. Trajmar, J. Phys. B6 (1973) L365.
[57] S.G. Lias, J. Phys. Chem. Ref. Data (Suppl. 1) 17 (1988) 272.
[58] E.N. Lassetre, A. Skerbele, M.A. Dillon, K.J. Ross, J. Chem. Phys. 48 (1968) 5066.
[59] I. Nenner, P.-M. Guyon, T. Baer, T.R. Govers, J. Chem. Phys. 72 (1980) 6587.
[60] H.M. Rosenstock, J. Phys. Chem. Ref. Data 6 (1977) 1.

[61] Y. Tanaka, A.S. Jursa, F.J. Le Blanc, J. Chem. Phys. 32 (1960) 1205.
[62] M.J. Weiss, S.R. Mielczarek, C.E. Kyuatt, J. Chem. Phys. 54 (1971) 1412.
[63] U. Gelius, J. Electron. Spectrosc. 5 (1974) 985.
[64] F.P. Larkins, J. Chem. Phys. 86 (1987) 3239.
[65] D.M.P. Holland, M.A. MacDonald, M.A. Hayes, Chem. Phys. 142 (1990) 291.
[66] D.A. Shaw, D.M.P. Holland, M.A. MacDonald, A. Hopkirk, M.A. Hayes, S.M. McSweeney, Chem. Phys. 163 (1992) 387.
[67] R.P. Wayne, Chemistry of Atmospheres, Oxford University Press, Oxford, 1991.
[68] G.J. Schulz, J. Chem. Phys. 34 (1961) 1778.
[69] D. Rapp, D.D. Briglia, J. Chem. Phys. 43 (1965) 1480.
[70] P.J. Chantry, J. Chem. Phys. 51 (1969) 3380.
[71] R.K. Curran, R.E. Fox, J. Chem. Phys. 34 (1961) 1590.
[72] A.V. Phelps, R.E. Voshall, J. Chem. Phys. 49 (1968) 4718.
[73] J.M. Warman, R.W. Fessenden, J. Chem. Phys. 49 (1968) 4718.
[74] J.L. Moruzzi, J.T. Dakin, J. Chem. Phys. 49 (1968) 5000.
[75] L. Sanche and G.J. Schultz, J. Chem. Phys. 58 (1973) 479.
[76] H. Shimarmori, R.W. Fessenden, J. Chem. Phys. 71 (1979) 3009.
[77] A. Zecca, I. Lazzizzera, M. Krauss, C.E. Kuyatt, J. Chem. Phys. 61 (1974) 4560.
[78] E.E. Ferguson, F.C. Fehsenfeld, A.L. Schmeltekopf, J. Chem. Phys. 47 (1967) 3085.
[79] J.N. Bardsley, J. Chem. Phys. 51 (1969) 3384.
[80] P.J. Chantry, J. Chem. Phys. 55 (1971) 2746.
[81] J.F. Paulson, Adv. Chem. Ser. 58 (1966) 28.
[82] J.F. Paulson, J. Chem. Phys. 52 (1970) 959.
[83] S.J. Nally, R.N. Compton, H.C. Schweinler, V.E. Anderson, J. Chem. Phys. 60 (1973) 4125.
[84] J.V. Coe, J.T. Snodgrass, C.B. Freidhoff, K.M. McHugh, K.H. Bowen, Chem. Phys. Lett. 124 (1986) 274.
[85] F.C. Fehsenfeld, E.E. Ferguson, J. Chem. Phys. 15 (1976) 1853.
[86] J. Dutton, F.M. Harris, D.B. Hughes, J. Phys. B8 (1975) 313.
[87] H. Sponer, L.G. Bonner, J. Chem. Phys. 8 (1940) 33.
[88] H.S. Johnston, G.S. Selwyn, Geophys. Res. Lett. 2 (1975) 549.
[89] R.D. Hudson, Can. J. Chem. 52 (1974) 1465.
[90] D.R. Bates, P.B. Hays, Planet. Space Sci. 15 (1967) 189.
[91] M. Zelikoff, K. Watanabe, E.C.Y. Inn, J. Chem. Phys. 21 (1953) 1643.
[92] L.C. Lee, M. Suto, J. Chem. Phys. 80 (1984) 4718.
[93] W.F. Chan, G. Cooper, C.E. Brion, Chem. Phys. 180 (1994) 77.
[94] T.C. Betts, V. McKoy, J. Chem. Phys. 60 (1974) 2947.
[95] S.D. Peyerimhoff, R.J. Buenker, J. Chem. Phys. 49 (1968) 2473.
[96] M. Shapiro, Chem. Phys. Lett. 46 (1977) 442.
[97] N.W. Winter, Chem. Phys. Lett. 33 (1975) 300.
[98] C. Fridh, L. Asbrink, E. Lindholm, Chem. Phys. 27 (1978) 169.
[99] A. Chutjian, G.A. Segal, J. Chem. Phys. 57 (1972) 3069.
[100] A.J. Bard, R. Parsons, J. Jordan, Standard Potentials in Aqueous Solution, Marcel Dekker, New York, 1985, p. 127.
[101] N.N. Greenwood, A. Earnshaw, Chemistry of the Elements, Pergamon Press, New York, 1984.
[102] G. Ritzoulis, J. Electroanal. Chem. 327 (1992) 209.
[103] G.A. Attard, A. Ahmadi, J. Electroanal. Chem. 389 (1995) 175.
[104] A. Ahmadi, E. Bracey, R.W. Evans, G. Attard, J. Electroanal. Chem. 350 (1993) 297.
[105] N. Furuya, H. Yoshiba, J. Electroanal. Chem. Interfacial Electrochem. 303 (1991) 271.
[106] H. Ebert, R. Parsons, G. Ritzoulis, T. Vandernoot, J. Electroanal. Chem. Interfacial Electrochem. 264 (1989) 181.
[107] K.E. Johnson, D.T. Sawyer, J. Electroanal. Chem. 49 (1974) 95.
[108] J.H.G. Van der Stegen, W. Visscher, J.G. Hoogland, Electrochem. Technol. 4 (1966) 564.
[109] B. Wang, X. Li, Anal. Chem. 70 (1998) 2181.
[110] A. Kudo, A. Mine, Appl. Surf. Sci. 121 (1997) 538.

[111] I. Taniguchi, T. Shimpuku, K. Yamashita, H. Ohtaki, J. Chem. Soc. Chem. Commun. (1990) 915.
[112] D.L. Ehman, D.T. Sawyer, J. Electronal. Chem. Interfacial Electrochem. 16 (1968) 541.
[113] N.N. Savodnik, V.A. Shepelin, T.I. Zalkind, Electrokhimiya 7 (1971) 424.
[114] N.N. Savodnik, V.A. Shepelin, T.I. Zalkind, Electrokhimiya 7 (1971) 583.
[115] I. Paseka, J. Vonkova, Electrochim. Acta 25 (1980) 1251.
[116] B.G. Snider, D.C. Johnson, Anal. Chim. Acta 105 (1979) 9.
[117] A. Rodes, R. Gomez, J.M. Orts, J.M. Feliu, J.M. Perez, A. Aldaz, Langmuir 11 (1995) 3549.
[118] D. Dutta, D. Landholt, Electrochem. Sci. Technol. 119 (1972) 1320.
[119] L.J.J. Janssen, M.M.J. Pieterse, E. Barendrecht, Electrochim. Acta 22 (1977) 27.
[120] M.J. Foral, S.H. Langer, Electrochim. Acta 36 (1991) 299.
[121] M.J. Foral, S.H. Langer, Electrochim. Acta 33 (1988) 257.
[122] S.H. Langer, K.T. Pate, Nature 284 (1980) 434.
[123] K.T. Pate, S.H. Langer, Environ. Sci. Technol. 19 (1985) 371.
[124] J.A. Colucci, M.J. Foral, S.H. Langer, Electrochim. Acta 30 (1985) 521.
[125] C.C. Delwiche, Denitrification, Nitrification, and Atmospheric Nitrous Oxide, Wiley, New York, 1981.
[126] C.S. Law, A.P. Rees, N.J.P. Owens, Estuar. Coast. Shelf Sci. 35 (1992) 301.
[127] C. Vankessel, D.J. Pennock, R.E. Farrell, Soil Sci. Soc. Am. J. 57 (1993) 988.
[128] O. Badr, S.D. Probert, Appl. Energy 42 (1992) 129.
[129] B.A. Averill, Chem. Rev. 96 (1996) 2951.
[130] S.S. Butcher, R.J. Charlson, G.H. Orians, G. Wolfe V, Global Biogeochemical Cycles, Academic Press, London, 1992.
[131] G. Stedman, Adv. Inorg. Chem. Radiochem. 22 (1979) 114.
[132] H.H. Sisler, in: R.B. King (Ed.), Encyclopedia of Inorganic Chemistry, Wiley, New York, 1994, p. 2516.
[133] A.G. Keenan, B. Dimitriades, J. Chem. Phys. 37 (1962) 1583.
[134] A.G. Keenan, K. Notz, N.B. Franco, J. Am. Chem. Soc. 91 (1969) 3168.
[135] W.A. Rosser, S.H. Inami, H. Wise, J. Phys. Chem. 67 (1963) 1753.
[136] C.I. Colvin, P.W. Fearnow, A.G. Keenan, Inorg. Chem. 4 (1965) 173.
[137] W.G. Sykes, R.H. Johnson, R.M. Hainer, Chem. Eng. Prog. 59 (1963) 66.
[138] H.B. Gray, J.D. Simon, W.C. Trogler, Braving the Elements, University Science Books, Sausalito, 1995.
[139] Y. Rozman, Russ. J. Inorg. Chem. 6 (1961) 399.
[140] Y.I. Rubtsov, I.I. Strizhevskii, A.I. Kazakov, E.B. Moshkovich, L.P. Andrienko, Zhur. Priklad. Khim. 62 (1989) 2417.
[141] J.V.R. Smit, Chem. Ind. (1964) 2018.
[142] C.W. Weston, in: M. Howe-Grant Jr. (Ed.), Encyclopedia of Chemical Technology, Wiley, New York, 1992, p. 698.
[143] J.M. MacNeil, H.T. Zhang, P.A. Berseth, W.C. Trogler, J. Am. Chem. Soc. 119 (1997) 9738.
[144] C.A. Bunton, E.A. Halevl, J. Chem. Soc. (1952) 4917.
[145] L.C.S. Melander, W.H. Saunders:, Reaction Rates of Isotopic Molecules, Wiley, New York, 1980.
[146] W.L. Marshall, R. Slusher, J. Inorg. Nucl. Chem. 37 (1975) 1191.
[147] A.D. Kelmers, L. Maya, D.N. Browning, W. Davis Jr., J. Inorg. Nucl. Chem. 41 (1979) 1583.
[148] C.I. Colvin, A.G. Keenan, J.B. Hunt, J. Chem. Phys. 38 (1963) 3033.
[149] J. Jander, U. Engelhardt, Developments in Inorganic Nitrogen Chemistry, vol. 2, Elsevier, New York, 1973.
[150] M.J. Thomas, A. Cummings, M. Gomez, Chemical Accident Investigation Report: Terra Industries, Inc. Nitrogen Fertilizer Facility, Port Neal, IA, USEPA, Region 7, 1996.
[151] H.W. Stephens, The Texas City Disaster 1947, University of Texas Press, Austin, TX, 1997.
[152] M.H. Thiemens, W.C. Trogler, Science 251 (1991) 932.
[153] D.D. Davis, in: W. Gerhartz (Ed.), Uhlman's Encyclopedia of Industrial Chemistry, VCH, Deerfield Beach, 1985.
[154] L.V. Pirutko, K.A. Dubkov, L.P. Solovyeva, G.I. Panov, Reac. Kinet. Catal. Lett. 58 (1996) 105.

[155] G.I. Panov, G.A. Sheveleva, A.S. Kharitonov, V.N. Romannikov, L.A. Vostrikova, Appl. Catal. A-Gen. 82 (1992) 31.
[156] E. Klemm, A. Reitzmann, S. Buchholz, H. Zanthoff, Chem. Ingen. Tech. 70 (1998) 1017.
[157] M. Hafele, A. Reitzmann, D. Roppelt, G. Emig, Appl. Catal. A-Gen. 150 (1997) 153.
[158] V.I. Sobolev, A.S. Kharitonov, Y.A. Paukshtis, G.I. Panov, J. Mol. Catal. 84 (1993) 117.
[159] V.I. Sobolev, K.A. Dubkov, E.A. Paukshtis, L.V. Pirutko, M.A. Rodkin, A.S. Kharitonov, G.I. Panov, Appl. Catal. A-Gen. 141 (1996) 185.
[160] A.S. Kharitonov, V.I. Sobolev, G.I. Panov, Uspekhi Khim. 61 (1992) 2062.
[161] M. Anpo, M. Matsuoka, K. Hano, H. Mishima, T. Ono, H. Yamashita, Korean J. Chem. Eng. 14 (1997) 498.
[162] J.N. Armor, T.A. Braymer, T.S. Farris, Y. Li, F.P. Petrocelli, E.L. Weist, S. Kannan, C.S. Swamy, Appl. Catal. B-Environ. 7 (1996) 397.
[163] A.D. Belapurkar, N.M. Gupta, G.M. Phatak, R.M. Iyer, J. Mol. Catal. 87 (1994) 287.
[164] B. Bonn, G. Pelz, H. Baumann, Fuel 74 (1995) 165.
[165] S. Bossmann, M. Ottaviani, T. Turek, Ber. Bun. Gesel. Phys. Chem. Chem. Phys. 101 (1997) 978.
[166] G. Centi, G. Cerrato, S. Dangelo, U. Finardi, E. Giamello, C. Morterra, S. Perathoner, Catal. Today 27 (1996) 265.
[167] G. Centi, A. Galli, B. Montanari, S. Perathoner, A. Vaccari, Catal. Today 35 (1997) 113.
[168] Y.F. Chang, J.G. Mccarty, Y.L. Zhang, Catal. Lett. 34 (1995) 163.
[169] J. Christopher, C.S. Swamy, React. Kinet. Catal. Lett. 39 (1989) 129.
[170] J. Christopher, C.S. Swamy, J. Mol. Catal. 62 (1990) 69.
[171] J. Christopher, C.S. Swamy, J. Mol. Catal. 68 (1991) 199.
[172] P. Ciambelli, A. DiBenedetto, E. Garufi, R. Pirone, G. Russo, J. Catal. 175 (1998) 161.
[173] R.S. Drago, K. Jurczyk, N. Kob, Appl. Catal. B-Environ. 13 (1997) 69.
[174] K. Eranen, N. Kumar, L.E. Lindfors, Appl. Catal. B-Environ. 4 (1994) 213.
[175] S. Imamura, T. Kitao, H. Kanai, S. Shono, K. Utani, H. Jindai, React. Kinet. Catal. Lett. 61 (1997) 201.
[176] U. Kameswari, J. Christopher, C.S. Swamy, React. Kinet. Catal. Lett. 41 (1990) 381.
[177] U. Kameswari, J. Christopher, C.S. Swamy, React. Kinet. Catal. Lett. 44 (1991) 31.
[178] C. Kodama, H. Orita, H. Nozoye, Appl. Surf. Sci. 121 (1997) 579.
[179] M. Kogel, V.H. Sandoval, W. Schwieger, A. Tissler, T. Turek, Chem. Eng. Technol. 21 (1998) 655.
[180] M. Kogel, V.H. Sandoval, W. Schwieger, A. Tissler, T. Turek, Chem. Ingen. Tech. 70 (1998) 878.
[181] C. Kordulis, H. Latsios, A. Lycourghiotis, P. Pomonis, J. Chem. Soc. Faraday Trans. 86 (1990) 185.
[182] T. Kubo, T. Ems, A. Atli, T. Aruga, N. Takagi, M. Nishijima, Surf. Sci. 382 (1997) 214.
[183] A.V. Kucherov, T.N. Kucherova, V.D. Nissenbaum, A.A. Slinkin, Kinet. Catal. 36 (1995) 673.
[184] K. Li, X. Wang, H. Zeng, Chem. Eng. Res. Des. 75 (1997) 807.
[185] J. Lin, H.Y. Chen, L. Chen, K.L. Tan, H.C. Zeng, Appl. Surf. Sci. 103 (1996) 307.
[186] A. Mascarenhas, H. Andrade, React. Kinet. Catal. Lett. 64 (1998) 215.
[187] M. Nakamura, H. Mitsuhashi, N. Takezawa, J. Catal. 138 (1992) 686.
[188] M. Nakamura, S.I. Fujita, N. Takezawa, Catal. Lett. 14 (1992) 315.
[189] M. Nakamura, H. Yanagibashi, H. Mitsuhashi, N. Takezawa, Bull. Chem. Soc. Jpn. 66 (1993) 2467.
[190] J.K. Oi, A. Obuchi, A. Ogata, H. Yagita, G.R. Bamwenda, K. Mizuno, Chem. Lett. (1995) 453.
[191] J. Oi, A. Obuchi, A. Ogata, G. Bamwenda, R. Tanaka, T. Hibino, S. Kushiyama, Appl. Catal. B-Environ. 13 (1997) 197.
[192] H. Orita, H. Kondoh, H. Nozoye, J. Catal. 177 (1998) 217.
[193] X.Y. Pang, H.C. Zeng, J.C. Wu, K. Li, Appl. Catal. B-Environ. 9 (1996) 149.
[194] G.I. Panov, V.I. Sobolev, A.S. Kharitonov, J. Mol. Catal. 61 (1990) 85.
[195] P. Pomonis, C. Kordulis, A. Lycourghiotis, J. Chem. Soc. Faraday Trans. 86 (1990) 711.
[196] M. Qian, H. Zeng, J. Mater. Chem. 7 (1997) 493.
[197] B.W. Riley, J.R. Richmond, Catal. Today 17 (1993) 277.
[198] V.I. Sobolev, A.S. Kharitonov, G.I. Panov, Dokl. Akad. Nauk SSSR 307 (1989) 1419.

[199] V.I. Sobolev, G.I. Panov, A.S. Kharitonov, V.N. Romannikov, A.M. Volodin, Kinet. Catal. 34 (1993) 797.
[200] V.I. Sobolev, G.I. Panov, A.S. Kharitonov, V.N. Romannikov, A.M. Volodin, K.G. Ione, J. Catal. 139 (1993) 435.
[201] C.S. Swamy, J. Christopher, Catal. Rev. Sci. Eng. 34 (1992) 409.
[202] T. Turek, J. Catal. 174 (1998) 98.
[203] J. Valyon, W.S. Millman, W.K. Hall, Catal. Lett. 24 (1994) 215.
[204] N. VanTuyen, I. Ikonnikov, A. Loginov, B. Romanovskii, Kinet. Catal. 38 (1997) 94.
[205] A.I. Vitvitskii, J. Appl. Chem. USSR 65 (1992) 1882.
[206] T. Yamashita, A. Vannice, J. Catal. 161 (1996) 254.
[207] K. Yuzaki, T. Yarimizu, S. Ito, K. Kunimori, Catal. Lett. 47 (1997) 173.
[208] V.L. Zholobenko, I.N. Senchenya, L.M. Kustov, V.B. Kazanskii, Kinet. Catal. 32 (1991) 132.
[209] V. Zholobenko, Mendeleev Commun. (1993) 67.
[210] A.S. Kharitonov, V.I. Sobolev, G.I. Panov, Kinet. Catal. 30 (1989) 1319.
[211] M. Kubota, K.J. Evans, C.A. Koerntgen, J.C. Marsters, J. Am. Chem. Soc. 100 (1978) 342.
[212] M. Kubota, K.J. Evans, C.A. Koerntgen, J.C. Marsters, J. Mol. Catal. 7 (1980) 481.
[213] K.S. Sun, K.C. Kong, C.H. Cheng, Inorg. Chem. 30 (1991) 1998.
[214] J.H. MacNeil, P.K. Gantzel, W.C. Trogler, Inorg. Chim. Acta 240 (1995) 299.
[215] J.H. MacNeil, P. Berseth, E.L. Bruner, T.L. Perkins, Y. Wadia, G. Westwood, W.C. Trogler, J. Am. Chem. Soc. 119 (1997) 1668.
[216] D. Gwost, K.G. Caulton, Inorg. Chem. 13 (1974) 414.
[217] B.F. Hoskins, F.D. Whillans, D.H. Dale, D.C. Hodgkin, Chem. Commun. (1969) 69.
[218] Y.A. Dorfman, V.S. Emel'yanova, B.O. Zhusupbekov, Kinet. Katal. 22 (1981) 375.
[219] J.A. Halfen, W.B. Tolman, J. Am. Chem. Soc. 116 (1994) 5475.
[220] J.A. Halfen, S. Mahapatra, M.M. Olmstead, W.B. Tolman, J. Am. Chem. Soc. 116 (1994) 2173.
[221] S. Mahapatra, J.A. Halfen, W.B. Tolman, J. Chem. Soc. Chem. Commun. (1994) 1625.
[222] P.P. Paul, K.D. Karlin, J. Am. Chem. Soc. 113 (1991) 6331.
[223] C.E. Ruggiero, S.M. Carrier, W.B. Tolman, Angew. Chem. Int. Ed. Engl. 33 (1994) 895.
[224] W.B. Tolman, Inorg. Chem. 30 (1991) 4877.
[225] G.B. Richter-Addo, P. Legzdins, Metal Nitrosyls, Oxford University Press, New York, 1992.
[226] E. Wegg-Aerssens, J.M. Tiedje, B.A. Averill, J. Am. Chem. Soc. 110 (1988) 6851.
[227] X.-J. Zhao, V. Sampath, W.S. Caughey, Biochem. Biophys. Res. Commun. 212 (1995) 1054.
[228] U.P. Singh, E. Obayashi, S. Takahashi, T. Iizuka, H. Shoun, Y. Shiro, Biochim. Biophys. Acta-Pro. Struc. Mol. Enzymol. 1384 (1998) 103.
[229] S.Y. Park, H. Shimizu, S. Adachi, A. Nakagawa, I. Tanaka, K. Nakahara, H. Shoun, E. Obayashi, H. Nakamura, T. Iizuka, Y. Shiro, Nat. Struc. Biol. 4 (1997) 827.
[230] E. Obayashi, K. Tsukamoto, S. Adachi, S. Takahashi, M. Nomura, T. Iizuka, H. Shoun, Y. Shiro, J. Am. Chem. Soc. 119 (1997) 7807.
[231] N. Toritsuka, H. Shoun, U.P. Singh, S.Y. Park, T. Iizuka, Y. Shiro, Biochim. Biophys. Acta-Protein Struc. Mol. Enzymol. 1338 (1997) 93.
[232] H. Shoun, T. Tanimoto, J. Biol. Chem. 266 (1991) 11078.
[233] J.H. MacNeil, P. Berseth, G. Westwood, W.C. Trogler, Environ. Sci. Technol. 32 (1998) 876.
[234] J.N. Armor, in: J.N. Armor (Ed.), Environmental Catalysis, American Chemical Society, Washington, DC, 1994, p. 2.
[235] M. Iwamoto, H. Hamada, Catal. Today 10 (1991) 57.
[236] S. Iwamoto, S. Shimizu, T. Inui, Stud. Surf. Sci. Catal. 84 (1994) 1523.
[237] M. Iwamoto, H. Yahiro, Catal. Today 22 (1994) 5.
[238] Y.P. Zhang, M. Flytzanistephanopoulos, J. Catal. 164 (1996) 131.
[239] R. Pirone, P. Ciambelli, G. Moretti, G. Russo, Appl. Catal. B-Environ. 8 (1996) 197.
[240] R.J. Wu, T.Y. Chou, C.T. Yeh, Appl. Catal. B-Environ. 6 (1995) 105.
[241] C.Y. Lee, K.Y. Choi, B.H. Ha, Appl. Catal. B-Environ. 5 (1994) 7.
[242] T. Mori, H. Yamamura, H. Ogino, H. Kobayashi, T. Mitamura, J. Am. Ceram. Soc. 77 (1994) 2771.
[243] G. Moretti, Catal. Lett. 23 (1994) 135.

[244] A. Ogata, A. Obuchi, K. Mizuno, A. Ohi, H. Ohuchi, J. Catal. 144 (1993) 452.
[245] M. Shelef, Catal. Lett. 15 (1992) 305.
[246] Y.J. Li, W.K. Hall, J. Catal. 129 (1991) 202.
[247] A. Ogata, A. Obuchi, K. Mizuno, A. Ohi, H. Aoyama, H. Ohuchi, Appl. Catal. 65 (1990) L11.
[248] Y.J. Li, W.K. Hall, J. Phys. Chem. 94 (1990) 6145.
[249] D.K. Liu, D.X. Shen, S.G. Chang, Environ. Sci. Technol. 25 (1991) 55.
[250] G. Centi, N. Passarini, S. Perathoner, A. Riva, in: J.N. Armor (Ed.), Environmental Catalysis, American Chemical Society, Washington, DC, 1994, p. 233.
[251] S.G. Chang, D.K. Liu, Nature 343 (1990) 151.
[252] S.G. Chang, G.C. Lee, Environ. Prog. 11 (1992) 66.
[253] E.K. Pham, S.G. Chang, Nature 369 (1994) 139.